Thermochimica Acta 510 (2010) 75–81

Contents lists available at ScienceDirect

Thermochimica Acta

journal homepage: www.elsevier.com/locate/tca

Crystal structure and thermoanalytical study of cobalt(II) and nickel(II) complexes with 2,2′-bis-(4,5-dimethylimidazole)

Simonetta De Angelis Curtis[a], Krystyna Kurdziel[b], Stefano Materazzi[a], Stefano Vecchio[c,*]

[a] Department of Chemistry, University of Rome "La Sapienza", P.le A. Moro 5, 00185 Roma, Italy
[b] Institute of Chemistry, Jan Kochanowski University of Humanities and Science, ..wi..tokryska 15 G, 25-406 Kielce, Poland
[c] Department of S.B.A.I., University of Rome "La Sapienza", Via del Castro Laurenziano 7, 00161 Roma, Italy

ARTICLE INFO

Article history:
Received 22 March 2010
Received in revised form 17 June 2010
Accepted 23 June 2010
Available online 30 June 2010

Keywords:
Cadmium(II) complexes
Imidazole derivatives
Crystal structure
TG
DTG
Coupled TG-MS
EGA
Decomposition kinetics

ABSTRACT

The crystal structure of two $[XL_3](NO_3)_2$ complexes, where X = Co(II), Ni(II); L = 2,2′-bis-(4,5-dimethylimidazole), were characterized by single crystal X-ray diffraction using SHELX-97. Thermogravimetry (TG) and evolved gas analysis by coupled mass spectrometry (EGA-MS) were used to study the thermal behaviour of both complexes. After dehydration, a multi-step decomposition occurred in the complexes examined due to the release of both the nitrate groups and the three ligand molecules. A final residue of the metal(II) oxides was found at 1073 K. A confirmation of the oxidative decomposition pattern initially proposed by the percentage mass loss data was obtained by the evolved gas analysis. Finally, data collected from TG experiments at different heating rates concerning the oxidative decomposition steps were processed using the Kissinger equation to obtain activation energy, pre-exponential factor and rate constant values at the middle of the experimental temperature range, while the dependence of activation energy from the degree of transformation was assessed using the isoconversional method of Ozawa–Flynn–Wall.

1. Introduction

The relevance of imidazole derivatives is due to the fact that imidazole ring is a moiety of histidine molecule and is a ligand toward transition metal ions for many biologically important molecules (i.e., non-heme systems and metallo proteins). Moreover, imidazoles are widely applied in a variety of fields ranging from pharmaceutics [1] to electrochemistry (e.g., as effective corrosion inhibitors or hidden curing agents for epoxy resins [2,3]) as well as in the field of thermo-luminescence [4]. The thermal behaviour of imidazole derivative complexes with divalent transition metal ions have been studied recently by different authors [5–7]. Spectral, magnetic and thermal behaviour of imidazole derivative complexes with divalent cadmium ions were also investigated using several techniques in conjunction with thermal analysis techniques [8–10]. In the recent years, a systematic experimental study concerning the synthesis, X-ray crystal structure characterization, thermal behaviour and kinetic investigation of the thermal decomposition processes occurring in imidazole derivative complexes with divalent transition metal ions was carried out by our research group [5,11–15]. As a follow-up of this research, the aim of this paper is to characterize the crystal structure and to investigate the thermal behaviour of the Co(II) and Ni(II) complexes with 2,2′-bis-(4,5-dimethylimidazole) (L), whose structural formulas is given below:

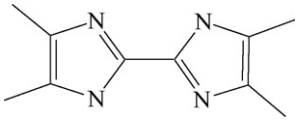

In this study different techniques were used: X-ray diffraction (XRD) spectroscopy, thermogravimetry (TG) and first-order thermogravimetry (DTG) and TG unit coupled with MS spectrometry (TG-MS). A possible degradation pathway is proposed for all the degradation steps according to the mass losses recorded by the TG unit, and a substantial confirmation is obtained by the TG-MS evolved gas analysis.

The kinetic methods proposed in this study are based on the assumption that kinetic parameters do not depend on the selected heating rate. The basic kinetic equation is as follows:

$$\frac{d\alpha}{dt} = k(T)f(\alpha) \quad (1)$$

where t is the time, α is the fraction decomposed defined as

$$\alpha = \frac{w_i - w_T}{w_i - w_f}, \quad (2)$$

* Corresponding author. Tel.: +39 06 4976 6906; fax: +39 06 4976 6749.
E-mail address: stefano.vecchio@uniroma1.it (S. Vecchio).

0040-6031/$ – see front matter © 2010 Elsevier B.V. All rights reserved.
doi:10.1016/j.tca.2010.06.025

$f(\alpha)$ is the model function, which assumes different mathematical forms depending on the reaction mechanism [16] and $k(T)$ is the specific rate constant, whose temperature dependence is commonly described by the Arrhenius equation:

$$k(T) = A\exp\left(-\frac{E}{RT}\right) \quad (3)$$

where E is the activation energy, A is the pre-exponential factor, R is the gas constant and T is the absolute temperature. Moreover, taking into account that under non-isothermal condition the heating rate β=dT/dt, dα/dt = dα/(dT/β), combining Eqs. (1) and (3), gives:

$$\frac{d\alpha}{dT} = \frac{A}{\beta}\exp\left(-\frac{E}{RT}\right)f(\alpha) \quad (4)$$

However, due to the complexity of the kinetic description concerning the solid state decomposition processes it is usually assumed that the activation energy is not a constant value but depends on α [17,18]. Therefore, in order to establish if such dependence exists or not, the kinetic procedure adopted in this work was firstly based on two multi-heating rate methods. Both approaches determine the activation energy using thermal analysis data carried out at different fixed heating rates without choosing a priori a defined model function. In particular, the first kinetic method used was Kissinger method [19] that uses the following equation:

$$\ln\left(\frac{\beta}{T_m^2}\right) = \ln\left(\frac{AR}{E}\right) - \left(\frac{E}{R}\right)\cdot\left(\frac{1}{T_m}\right) \quad (5)$$

where T_m should be the DTA or DSC peak temperature at a given heating rate β. However, the DTG peak temperature (denoted with the same symbol) should provide the same information unless the heat released by reaction changes with α [20]. From the slope of Eq. (5) a single activation energy value for each step of mass loss is given. In order to test the dependence of activation energy on the fraction decomposed α the isoconversional method of Ozawa–Flynn–Wall (OFW) [21,22] was also considered. This method is based on the integral form of Eq. (1) according to the following isoconversional equations:

$$\ln\beta = \ln\left(\frac{A_\alpha R}{E_\alpha}\right) - \ln g(\alpha) - 5.3305 - 1.052\left(\frac{E_\alpha}{R}\right)\left(\frac{1}{T_\alpha}\right). \quad (6)$$

Once the Doyle's approximation [23]: $\ln p(x) \approx -5.3305 - 1.052x$, where $x = E_\alpha/(RT_\alpha)$ and $20 \le x \le 60$) is verified to be valid over the entire range of α, then at any selected value of α determined from TG data using Eq. (2), the corresponding E_α value is derived from the slope of each regression straight line derived by the $\ln\beta$ *vs.* $1/T_\alpha$ plot.

2. Materials and methods

2.1. Materials

To a suspension of 2 mmol (0.38045 g) of 2,2′-bis-(4,5-dimethylimidazole) in 20 cm^3 of methanol, a solution containing 1 mmol of nitrate(V) cobalt(II) or nickel(II) in 20 cm^3 of the same solvent was gradually added stirring all the time. As a result of the reaction, the suspension dissolved and a clear solution was formed. The solution was left at room temperature to crystallize. After a few days crystalline complexes of 2,2′-bis-(4,5-dimethylimidazole) with cobalt(II) orange in color and with nickel(II) green in color precipitated from the solutions. Results of the elemental analyses are as follows: cobalt(II) complex: C, 47.9; H, 5.5; N, 26.0; calc. for $[CoL_3](NO_3)_2$; C, 47.81; H, 5.62; N, 26.02%. Nickel(II) complex C, 47.6; H, 5.7; N, 25.9; calc. for $[NiL_3](NO_3)_2$; C, 47.82; H, 5.60; N:26.02%.

2.2. Methods

Elemental analyses were run on a Vario EL III (Kendro). The IR spectra were recorded on a Perkin Elmer 180 (spectral range 50–4000 cm^{-1}) spectrophotometer in Nujol and in KBr pellets.

X-ray measurements were performed on a Kuma KM4CCD diffractometer. The structures were solved by direct methods using the SHELX-97 [24] and refined by full-matrix least-squares methods using the SHELXL-97 [25] programme. Details of the crystal data and refinement for the present compounds are collected in Table 1.

The TG curves were recorded using a Perkin-Elmer TGA7 equipment in the temperature range between 293 and 1073 K, the atmosphere was pure nitrogen or air (gaseous mixture of nitrogen and oxygen with 80 and 20%, v/v, respectively) under a flow rate of 100 mL min^{-1}; for the kinetic study TG experiments were carried out using 2–3 mg of sample at several heating rates (2.5, 5, 10 and 20 K min^{-1}), while the thermal behaviour was investigated using TG data at 10 K min^{-1} because of its best resolution. Mass spectra of the gases evolved during the experiments were recorded by a simultaneous TG/DTA apparatus (STD 2960 Simultaneous DTA–TGA, TA Instruments Inc., USA) using sealed crucibles with a pinhole on the top. The gaseous species were analyzed by a ThermoStar GDS 200 (Balzers Instruments) quadrupole mass spectrometer equipped with Chaneltron detector, through a heated 100% methyl deactivated fused silica capillary tubing. Data collection was carried out with QuadStar 422v60 software in multiple ion detection mode (MID) monitoring 64 selected channels ranging mostly between 12 and 78 m/z.

3. Results and discussion

3.1. Crystal structure and infrared spectra

Fig. 1 shows the molecular structure and the numeration of atoms in the Co(II) and Ni(II) complex ions with 2,2′-bis-(4,5-dimethylimidazole). The packing of complex $[NiL_3](NO_3)_2$ in a unit cell is given in Fig. 2. Selected bond lengths and angles are shown in Table 2.

In both complexes the coordination cation $[ML_3]^{2+}$ (M = Co(II) or Ni(II)) is made up of a metal ion and three molecules of 2,2′-bis-(4,5-dimethylimidazole) (L) which is a chelating ligand connected with the central ion via 'pyridine' nitrogen atoms of imidazole rings. As a result of these interactions, local molecular CoN_6 and NiN_6 chromophores are formed. The structural data show that a distorted octahedron describes the geometry of the coordination sphere of both complexes.

The coordination of bidetante 2,2′-bis-(4,5-dimethylimidazole) molecules results in the formation of five-membered chelate rings. Nitrogen–metal–nitrogen bond angles of these rings are 78.4(2)°, 78.5(2)°, 78.9(2)° in the cobalt (II) complex and 80.0(2)°, 80.0(2)°, 79.4(2)° in the nickel(II) complex. Analogous angles in compounds of nickel(II) with bipyridine $[Ni(bpy)_3]^{2+}$ [26] and 2,2′-phenanthroline $[Ni(fen)_3]^{2+}$ are similar and are 79° [27]. In compounds of 2,2′-bis-(4,5-dimethylimidazole) with Cu(II) – $\{[Cu(Me_4diim)_2ONO_2](NO_3)\}$ these angles are 80.8(2)° and 88.1(2)° whereas in the $[Cu_{0,1}Zn_{0,9}(Me_4diim)_2]\cdot(NO_3)_2$ complex they are 81.4(2)° and 81.5(2)° [28].

Such small N–metal–N chelate angles should cause an increase in other angles around the cobalt(II) and nickel(II) ions. The angles of the cobalt(II) and nickel(II) complexes are within 90.2(2)–96.0(2)° and 90.5(2)–95.1(3)°, respectively.

Cobalt(II)–nitrogen and nickel(II)–nitrogen coordination bonds of the complexes are within the ranges of

Table 1
Crystal data and structure refinement for $[CoL_3](NO_3)_2$ and $[NiL_3](NO_3)_2$ complexes.

	$[CoL_3](NO_3)_2$	$[NiL_3](NO_3)_2$
Empirical formula	$C_{30}H_{42}N_{14}CoO_6$	$C_{30}H_{42}N_{14}NiO_6$
Molar mass (g mol^{-1})	753.71	753.49
Temperature (K)	100(1)	100(1)
Radiation	Mo Kα (λ = 0.71073 Å)	Mo Kα (λ = 0.71073 Å)
Crystal system	Trigonal/hexagonal	Trigonal/hexagonal
Space group	P3(2)	P3(2)
a (Å)	13.758(2)	13.763(2)
b (Å)	13.758(2)	13.763(2)
c (Å)	16.686(3)	16.474(2)
V (Å^3)	2735.2(8)	2702.5(6)
Z, calculated density (Mg m^{-3})	3, 1.373	3, 1.389
Absorption coefficient (mm^{-1})	0.532	0.601
F(0 0 0)	1185	1188
Crystal size (mm)	0.18 × 0.18 × 0.20	0.15 × 0.20 × 0.20
2θ range (°)	3.63–24.99	3.42–24.99
Index ranges	$-16 \le h \le 16$, $-16 \le k \le 16$, $-19 \le l \le 10$	$-16 \le h \le 16$, $-16 \le k \le 16$, $-19 \le l \le 13$
Reflections collected/unique	15704/4554 [*R*(int) = 0.0459]	14892/4580 [*R*(int) = 0.0596]
Completeness to 2θ = 24.99	99.7%	99.7%
Data [*I* > 2sigma(*I*)]/parameters	3320/472	2981/472
Goodness-of-fit on F^2	1.002	0.993
Final *R* indices [*I* > 2sigma(*I*)]	R_1 = 0.0581, wR_2 = 0.1272	R_1 = 0.0622, wR_2 = 0.1214
R indices (all data)	R_1 = 0.0828, wR_2 = 0.1400	R_1 = 0.1029, wR_2 = 0.1391
Absolute structure parameter	0.01(2)	0.04(2)
Largest diff. peak and hole	0.367 and −0.187e. Å^{-3}	0.340 and −0.224 e. Å^{-3}

2.123(6)–2.172(5) Å and 2.079(7)–2.129(6) Å, respectively. However, metal–nitrogen bonds in the above-mentioned copper(II) and zinc(II) complexes are within the following ranges: Cu–N, 1.987–2.210 Å; Zn–N, 2.058–2.103 Å, respectively.

Nitrate groups are beyond the coordination sphere of central ions. They are connected with the coordination $[ML_3]^{2+}$ cation by hydrogen bonds. These bonds form oxygen atoms with hydrogen atoms of pyrrole nitrogen atoms (–NH). Lengths of these bonds are given in Tables 3 and 4.

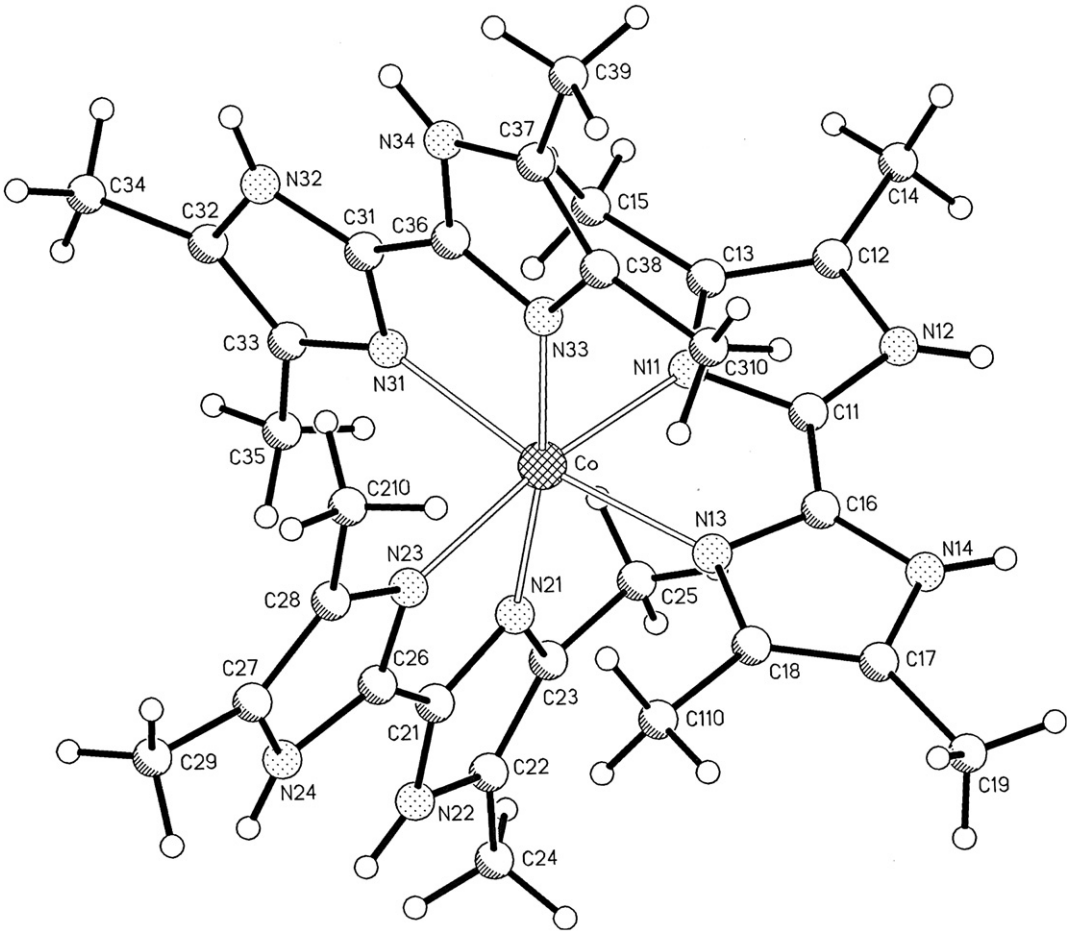

Fig. 1. The structure and numbering scheme of $[CoL_3](NO_3)_2$.

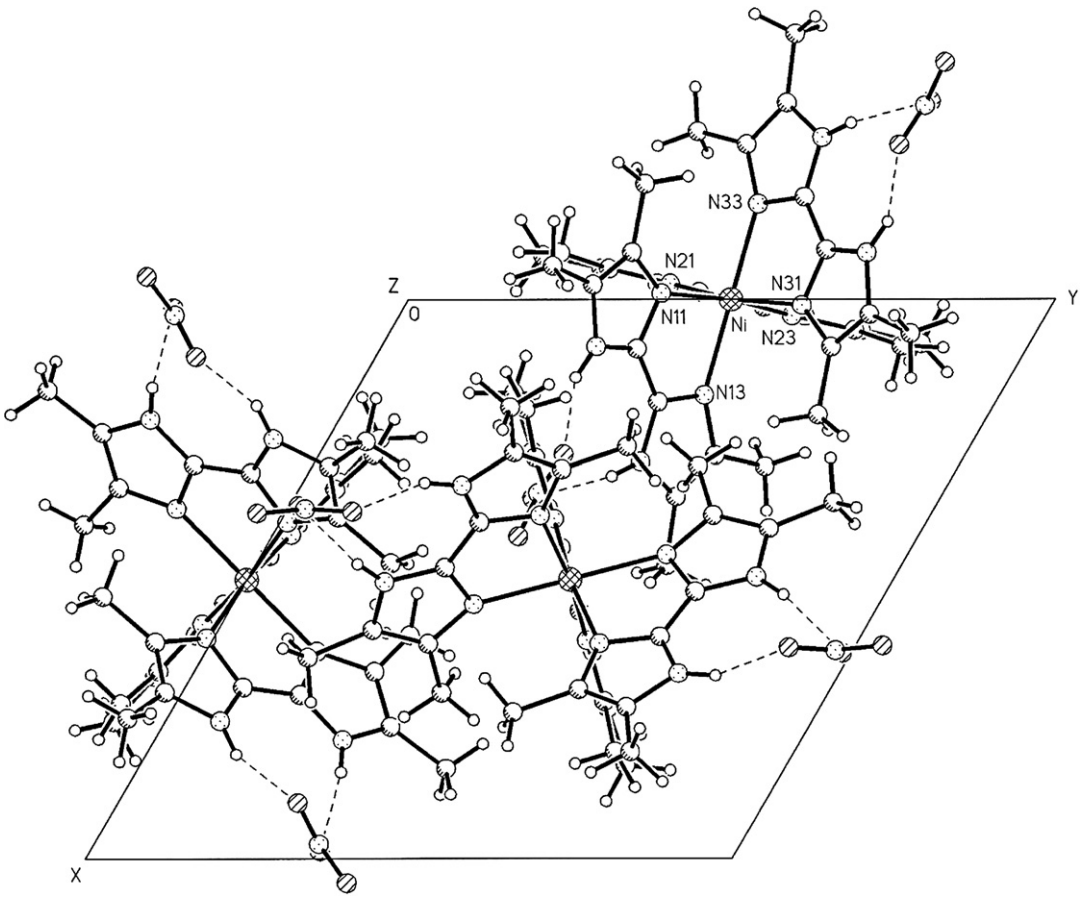

Fig. 2. Molecular packing of $[NiL_3](NO_3)_2$ in the unit cell.

The contribution of pyrrole hydrogen atoms in a hydrogen bond is reflected in infrared absorption spectra. In free 2,2′-bis-(4,5-dimethylimidazole) a strong and broad band with its maximum at ~2800 cm^{-1} is attributed to the –NH group and intermolecular N–H···N hydrogen bonds. In the cobalt(II) and nickel(II) complexes studied here this band is shifted towards higher frequencies, about 3100 cm^{-1}, as a result of the disruption of N–H···N hydrogen bond network of free ligand and the formation of new inter- and intramolecular N–H···O hydrogen bonds.

Lengths of nitrogen–oxygen bonds in nitrate groups are within the range of 1.11(1)–1.29(1) Å, whereas angles of the oxygen–nitrogen–oxygen bonds are within 117.2(7)–123.3(7)° in the cobalt(II) complex and within 115.4(8)–123.7(9) in the nickel(II) complex.

Table 2
Selected bond lengths (Å) and angles (°) for $[CoL_3](NO_3)_2$ and $[NiL_3](NO_3)_2$ complexes.

	Bond lengths (Å)			Bond angles (°)	
	$[CoL_3](NO_3)_2$	$[NiL_3](NO_3)_2$		$[CoL_3](NO_3)_2$	$[NiL_3](NO_3)_2$
M–N(31)	2.123(6)	2.113(6)	N(31)–Co–N(33)	78.9(2)	79.4(2)
M–N(33)	2.125(6)	2.129(6)	N(31)–Co–N(13)	170.8(2)	95.0(2)
M–N(13)	2.149(5)	2.127(6)	N(33)–Co–N(13)	95.8(2)	172.1(2)
M–N(21))	2.150(5)	2.080(7)	N(31)–Co–N(21)	96.0(2)	171.4(3)
M–N(23)	2.163(5)	2.079(7)	N(33)–Co–N(21)	170.7(2)	93.7(2)
M–N(11)	2.172(5)	2.104(6)	N(13)–Co–N(21)	90.2(2)	92.4(2)
O(1)–N(1)	1.199(9)	1.166(10)	N(31)–Co–N(23)	92.5(2)	95.1(3)
O(2)–N(1)	1.266(8)	1.109(8)	N(33)–Co–N(23)	93.8(2)	92.6(2)
O(3)–N(1)	1.142(7)	1.276(10)	N(13)–Co–N(23)	95.3(2)	93.4(2)
O(4)–N(2)	1.205(9)	1.172(10)	N(21)–Co–N(23)	78.5(2)	80.0(3)
O(5)–N(2)	1.139(7)	1.288(10)	N(31)–Co–N(11)	94.3(2)	90.5(2)
O(6)–N(2)	1.263(8)	1.116(9)	N(33)–Co–N(11)	92.7(2)	94.5(2)
			N(13)–Co–N(11)	78.4(2)	80.0(2)
			N(21)–Co–N(11)	95.5(2)	95.1(2)
			N(23)–Co–N(11)	171.3(2)	171.6(3)
			O(2)–N(1)–O(1)	119.2(7)	123.7(9)
			O(3)–N(1)–O(1)	123.1(7)	120.6(9)
			O(2)–N(1)–O(3)	117.5(7)	115.5(8)
			O(6)–N(2)–O(4)	119.3(7)	123.6(10)
			O(5)–N(2)–O(4)	123.3(7)	120.9(9)
			O(6)–N(2)–O(5)	117.2(7)	115.4(8)

Table 3
Hydrogen bond lengths (Å) and angles (°) for $[CoL_3](NO_3)_2$ complex.

D–H...A	d(D–H)	d(H...A)	d(D...A)	<(DHA)
N(12)–H(12)...O(4)	0.86	1.99	2.836(9)	167.6
N(14)–H(14)...O(5)	0.86	2.01	2.803(8)	152.9
N(22)–H(22)..O(3)	0.86	2.00	2.797(9)	153.6
N(24)–H(24)...O(1)	0.86	1.99	2.838(9)	168.0
N(32)–H(32)...O(6)*a*	0.86	2.03	2.848(10)	158.4
N(32)–H(32)...O(5)a	0.86	2.55	3.225(9)	136.2
N(34)–H(34)...O(2)*b*	0.86	2.04	2.857(9)	158.0
N(34)–H(34)...O(3)*b*	0.86	2.56	3.232(9)	136.3

Symmetry transformations used to generate equivalent atoms: $a = -y+2, x-y+1, z+2/3b = -y+1, x-y, z+2/3$

Table 4
Hydrogen bond lengths (Å) and angles (°) for $[NiL_3](NO_3)_2$ complex.

D–H...A	d(D–H)	d(H...A)	d(D...A)	<(DHA)
N(12)–H(12)...O(2)	0.86	2.00	2.805(10)	155.8
N(14)–H(14)...O(1)	0.86	1.99	2.833(10)	166.9
N(22)–H(22)...O(5)a	0.86	2.02	2.846(11)	159.8
N(22)–H(22)...O(6)a	0.86	2.54	3.217(10)	136.1
N(24)–H(24)...O(3)b	0.86	2.03	2.848(11)	158.8
N(24)–H(24)...O(2)b	0.86	2.53	3.215(10)	136.6
N(32)–H(32)...O(6)	0.86	2.00	2.800(10)	154.7
N(34)–H(34)...O(4)	0.86	1.99	2.837(10)	167.0

Symmetry transformations used to generate equivalent atoms: $a = -x+y-1, -x, z-2/3b = -x+y, -x+1, z-2/3$.

The nitrate group is signaled by three characteristic bands in the IR spectrum. A strong band is observed at 1368 cm^{-1} and two others, weak, are at 1068 and 832 cm^{-1}.

3.2. Thermal, evolved gas and kinetic analyses

Three steps of mass loss are shown in the TG/DTG curves of the complexes examined (Fig. 3), the first of which occurred up to 373 K with the release of about 1–2% (w/w) of water (Table 5). In the range between 473 and 595 K, the second step is attributable for both complexes to the loss of both the nitrate groups similarly to what it has been previously described for other imidazole

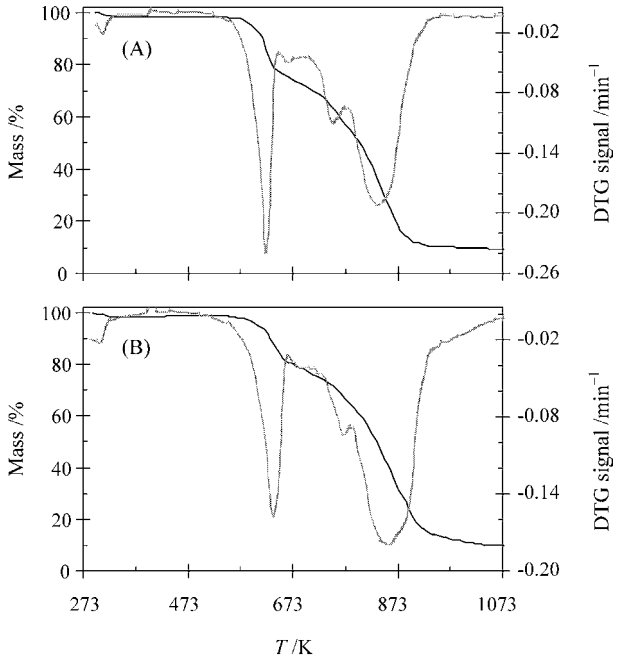

Fig. 3. TG (—) and DTG (—) curves of the complex: (A) $[CoL_3](NO_3)_2$ and (B) $[NiL_3](NO_3)_2$. Heating rate: 10K min^{-1}; air flow at 100 mL min^{-1} rate.

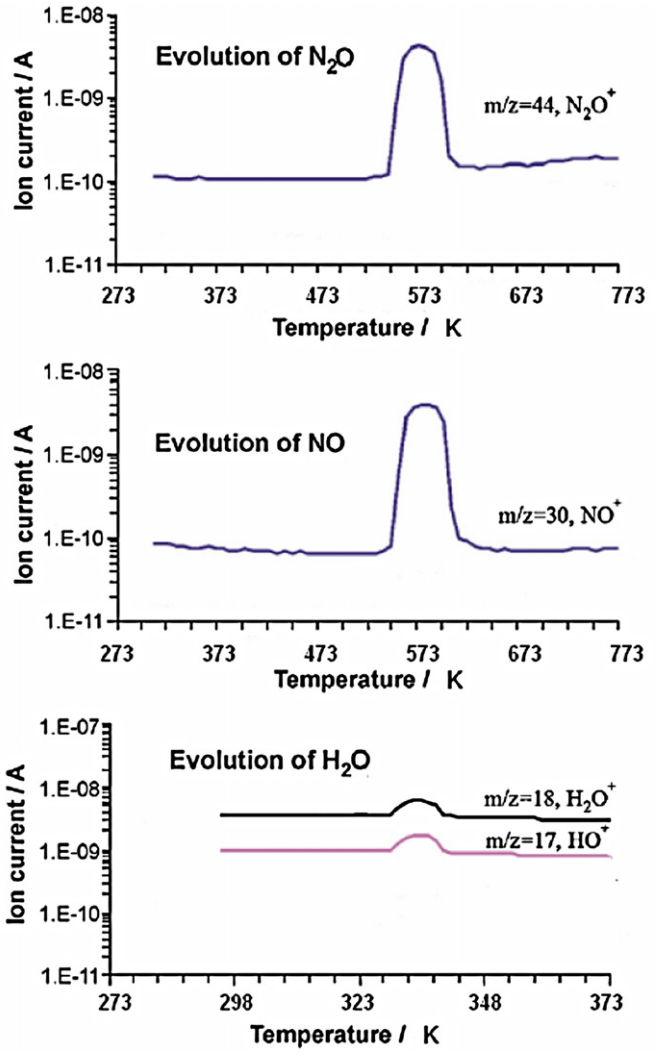

Fig. 4. Gas evolution curves of the gaseous species, represented by their characteristic mass spectroscopic ion fragments, for the thermal decomposition processes of the complex $[CoL_3](NO_3)_2$.

derivative complexes [3,29], which have nitrate groups inside or outside the coordination sphere of the central atom. Three 2,2′-bis-(4,5-dimethylimidazole) molecules are released in the third step between 673 and 973 K as three overlapped processes. At 1073 K a final residue of Co and NiO can be considered on the basis of the fair agreement between the experimental and predicted mass loss percentages given in Table 5 and confirmed by the X-ray diffraction spectra (not shown) carried out on a sample treated at 1000 °C. A good agreement between the experimental and predicted mass loss percentages given in Table 5 is also found for the second and third steps related to nickel(II) complex, while only slight differences are observed in the case of the cobalt(II) complex, thus substantially confirming the reliability of the thermal decomposition patterns suggested for both compounds.

The results obtained using the TG-MS measurements, summarized in Table 5, enable the thermal decomposition pattern scheme proposed to be confirmed. In fact, Fig. 4 shows the TG-MS gas analysis representing the evolved gas characterization, which clearly evidenced the fragments due to the loss of the water and then of the nitrate groups.

As far as the kinetic analysis of decomposition processes is concerned, from the slopes and intercepts of a regression line applied to Eq. (5) single values of activation energies and pre-exponential

Table 5
Results of the TG and TG/FTIR evolved gas analysis.

Complex	Step	ΔT (K)	Mass loss (%)		Fragments	Mechanism hypothesized
			Calc.	Found	m/z	
$[CoL_3](NO_3)_2$	I	298–373		1.4	17–18	Dehydration
	II	493–600	16.5[a]	21.5	30–44	Release of two nitrate groups
	III	600–763	75.7[b]	69.0		Release of three ligand moieties
	Residue	298–1073	7.8[c]	8.1		
$[NiL_3](NO_3)_2$	I	25–100		1.8	17–18	Dehydration
	II	473–595	16.5[a]	15.5	30–44	Release of two nitrate groups
	III	595–783	75.8[b]	72.7		Release of three ligand moieties
	Residue	298–1073	9.9[d]	10.0		

The errors associated with the mass loss percentages found were estimated to be lower than 5%.
[a] Theoretically predicted on the basis of the release of two NO_3 moieties.
[b] Theoretically predicted on the basis of the release of three L moieties.
[c] Theoretically predicted on the basis of the metal(II) as residue.
[d] Theoretically predicted on the basis of the metal(II) oxide as residue.

Table 6
Regression and Arrhenius parameters for the decomposition processes by the Kissinger method.

Complex	Step	$\ln(\beta/T_m^2) = a + b \times 10^3 \times T_m^{-1}$		R^2	E (kJ mol^{-1})[a]	$\ln(A/\text{min}^{-1})$[a]	$\langle T \rangle$ (K)	$\ln(k(\langle T \rangle)/\text{min}^{-1})$[a]
		a[a]	b (K)[a]					
$[CoL_3](NO_3)_2$	II	26.8 ± 3.5	-22.8 ± 2.1	0.9835	189 ± 17	37 ± 3	877	0.94 ± 0.08
	III	3.6 ± 1.5	-11.8 ± 1.2	0.9807	98 ± 10	13 ± 1	1064	0.25 ± 0.02
$[NiL_3](NO_3)_2$	II	20.4 ± 5.4	-19.4 ± 3.3	0.9444	161 ± 28	30 ± 5	893	0.75 ± 0.13
	III	1.8 ± 0.2	-10.5 ± 0.2	0.9993	88 ± 2	11.0 ± 0.2	1074	0.215 ± 0.004

[a] The associated uncertainty are standard deviations.

factors are calculated for the second and third steps of both complexes studied. All these values are reported in Table 6 along with the mean of the experimental temperature range, $\langle T \rangle$, and the logarithm of the rate constant values, $\ln(k(\langle T \rangle)/\text{min}^{-1})$, calculated at this temperature using the Arrhenius equation. The Arrhenius parameters (activation energy pre-exponential factor) for the thermal release of the nitrate groups of the Cobalt(II) complex are slightly higher than those of the Nickel(II) complex even if the difference of E and $\ln A$ values are comparable with the associated uncertainties. Similar results are obtained for the thermal release of the ligand molecules, where the Arrhenius parameters are significantly lower than those related to the previous step: the difference is about 80–90 kJ mol^{-1} and 24–29 for E and $\ln(A/\text{min}^{-1})$ values, respectively. In order to reveal the complexity of multi-step processes like thermal decompositions, the change of activation energy with the fraction decomposed α was determined using Eq. (6) for each decomposition step. The conversion E- and temperature-dependence plots for the second ($\alpha \leq 0.25$) and third ($0.3 < \alpha < 0.95$) steps of mass loss of both complexes were given in Fig. 5. As far as the second step of mass loss is concerned, the comparison between these values and those obtained with the Kissinger method (dotted lines) is not satisfactory for the $[CoL_3](NO_3)_2$ complex (isoconversional E values in Fig. 5A lie outside the range of values determined by the Kissinger method), while is better in the case of the $[NiL_3](NO_3)_2$ complex (Fig. 5B). On the contrary, the agreement among the activation energy values concerning the third step of mass loss is excellent for both complexes (the isoconversional values lie inside the ranges of Kissinger values delimited by the dotted lines in Figs. 5A and B).

However, the values of Arrhenius parameters are not suitable to establish a stability order between the two complexes: processes with higher activation energy and higher pre-exponential factor are contradictory, because the former should corresponds to lower stability, while the latter should correspond to higher stability. Therefore, in order to establish which the rate determining decomposition step is, the rate constants $k(\langle T \rangle)$ for all decomposition steps were calculated at the average of the experimental temperature range investigated ($\langle T \rangle$) using the Arrhenius equation. The derived $k\langle T \rangle$ values for both decomposition processes of both complexes were compared in Table 6, where the rate determining step seems to be the third one attributed to the thermal

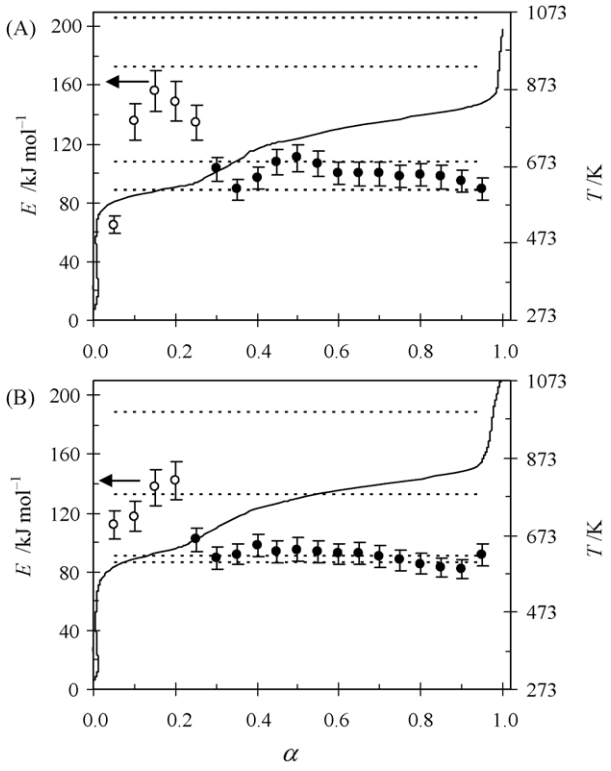

Fig. 5. Conversion α-dependence of activation energy and temperature (at 10 K min^{-1}) for the second (white circles) and third (black circles) steps of mass loss for the complex: (A) $[CoL_3](NO_3)_2$ and (B) $[NiL_3](NO_3)_2$. The ($E \pm$ associated uncertainties) values determined with the Kissinger method are given as dotted lines.

release of the three ligand molecules: the *k*<*T*> values associated to the second step of both complexes, ascribed to the release of two nitrate groups, are about twice those related to the third step, which can be considered equivalent for both complexes. As a consequence, comparable thermal stabilities may be assessed for both the complexes considered in this study. This result can be considered largely expected on the basis of the similar thermal profiles of TG, DTG and DSC found for the two complexes examined.

4. Conclusions

The crystal structures of cobalt(II) and nickel(II) complexes with 2,2′-bis-(4,5-dimethylimidazole) were characterized by single crystal X-ray diffraction and infrared spectra. The structural data obtained in this study are able to point out the following concluding remarks: (i) a distorted octahedron describes the geometry of the coordination sphere of both complexes, (ii) the coordination of bidetante 2,2′-bis-(4,5-dimethylimidazole) molecules results in the formation of five-membered chelate rings, (iii) nitrate groups are beyond the coordination sphere of central ions and (iv) disruption of N–H···N hydrogen bond network of free ligand and formation of new inter- and intramolecular N–H···O hydrogen bonds.

The thermal behaviour as well as the decomposition pathways along with the associated kinetic characteristics of the two complexes was studied using thermoanalytical techniques. The promising results obtained in the present study along with those reported during the last five years will enable us to provide in the near future an exhaustive survey on the structural and thermoanalytical characterization of 1-allylimidazole and other imidazole derivatives complexes with different transition metal ions.

Supplementary data

Detailed crystal data and structure refinement for $[CoL_3](NO_3)_2$ and $[NiL_3](NO_3)_2$ have been deposited with the Cambridge Crystallographic Data Centre under No. 723951 and CCDC 723952, respectively. Copies of this information may be obtained free of charge from The Director, CCDC, 12 Union Road, Cambridge, CB2 IEZ, UK (fax: +44 1223 336033; e-mail: deposit@ccdc.cam.ac.uk or http://www.ccdc.cam.ac.uk).

Acknowledgements

Authors wish to thank the Italian M.I.U.R. for its financial support.

References

[1] J.M. Rieder, J. Lepschy, Tetrahedron Lett. 43 (2002) 2375–2376.
[2] G. Bereket, C. Ogretir, A. Yurt, J. Mol. Struct.: Theochem. 571 (2001) 139–145; G. Bereket, E. Hur, C. Ogretir, J. Mol. Struct.: Theochem. 578 (2002) 79–88.
[3] V.I. Kalmykov, V.A. Ivanov, Zh. Prikl. Khim. 52 (1979) 889–893.
[4] Z. Fang, S. Wang, Z. Lei, X. Zuxun, R. Jun, W. Xianbao, Y. Qiongfeng, Mater. Chem. Phys. 107 (2008) 305–309.
[5] K. Kurdziel, T. Glowiak, S. Materazzi, J. Jezierska, Polyhedron 22 (2003) 3123–3128.
[6] M. Olczak-Kobza, R. Czylkowski, J. Karolak-Wojciechowska, J. Therm. Anal. Calorim. 74 (2003) 895–904.
[7] W. Wolodkiewicz, J. Therm. Anal. Calorim. 68 (2002) 141–146.
[8] O.Z. Yeşilel, H. Ölmez, H. Içbudak, J. Therm. Anal. Calorim. 89 (2007) 555–559.
[9] M. Arshad, A.H. Qureshi, S. Rehman, K. Masud, J. Therm. Anal. Calorim. 89 (2007) 561–566.
[10] P. Naumov, V. Jordanovska, B. Boyanov, G. Jovanovski, J. Therm. Anal. Calorim. 66 (2001) 469–477.
[11] S. De Angelis Curtis, S. Materazzi, K. Kurdziel, S. Vecchio, J. Therm. Anal. Calorim. 92 (2008) 109–114.
[12] S. Materazzi, S. Aquili, S. De Angelis Curtis, S. Vecchio, K. Kurdziel, F. Sagone, Thermochim. Acta 421 (2004) 19–24.
[13] S. Vecchio, S. Materazzi, K. Kurdziel, Int. J. Chem. Kinet. 37 (2005) 667–674.
[14] S. Materazzi, S. Aquili, S. Vecchio, K. Kurdziel, Thermochim. Acta 457 (2007) 7–10.
[15] S. De Angelis Curtis, M. Kubiak, K. Kurdziel, S. Materazzi, S. Vecchio, J. Anal. Appl. Pyrol. 87 (2010) 175–179.
[16] X. Gao, D. Chen, D. Dollimore, Thermochim. Acta 223 (1993) 75–82.
[17] S. Vyazovkin, C.A. Wight, Ann. Rev. Phys. Chem. 48 (1997) 125–149.
[18] A.K. Galwey, M.E. Brown, Thermal Decomposition of Ionic Solids, Elsevier, Amsterdam, 1999.
[19] H.E. Kissinger, Anal. Chem. 29 (1957) 1702–1706.
[20] J. Dweck, R.S. Aderne, D.J. Shanfield, J. Therm. Anal. Calorim. 64 (2001) 1163–1169.
[21] J.H. Flynn, L.A. Wall, J. Res. Natl. Bur. Stand. Sect. A 70 (1966) 487–523.
[22] T. Ozawa, Bull. Chem. Soc. Jpn. 38 (1965) 1881–1886.
[23] C.D. Doyle, J. Appl. Polym. Sci. 6 (1962) 639–642.
[24] G.M. Sheldrick, SHELXS 97, Program for Solution of Crystal Structure, University of Gőttingen, Germany, 1997.
[25] G.M. Sheldrick, SHELXL 97, Program for Refinement of Crystal Structure, University of Gőttingen, Germany, 1997.
[26] E.E. Bernarducci, P.K. Bharadwaj, R.A. Lalancette, K. Krogh-Jespersen, J.A. Potenza, H.J. Schugar, Inorg. Chem. 22 (1983) 3911–3920.
[27] A. Wada, N. Sakabe, J. Tanaka, Acta Crystallogr. B 32 (1976) 1121–1127.
[28] B.A. Frenz, J.A. Ibers, Inorg. Chem. 11 (1972) 1109–1116.
[29] S. Materazzi, K. Kurdziel, U. Tentolini, A. Bacaloni, S. Aquili, Thermochim. Acta 395 (2003) 133–137.